A GROUND-HUGGING DOWNRANGE VAPOR CLOUD DUE TO OBLIQUE IMPACTS. T. Hamura[1] , K. Kurosawa[2], S. Hasegawa[2], and S. Sugita[1], [1]Dept. of Complexity Sci. & Eng., Univ. of Tokyo (Kashiwanoha, Kashiwa, Chiba 277-8561, JAPAN, tiger@astrobio.k.u-tokyo.ac.jp), [2]ISAS/JAXA (Yoshinodai, Sagamihara, Kanagawa, 252-5210).

Introduction: A number of planetary exploration missions showed that planets/satellites with solid surface were suffered intense meteoritic bombardment at 3.8-4.6 Gyr ago [e.g., 1]. A large fraction of impactors collide with the planets/satellites obliquely [2]. In oblique impacts, impact-induced vapor clouds are divided into the 2 components; a downrange moving component and a hemispherical expanding one from the impact point [3]. If the planet has a thick atmosphere like Venus and Earth, complex atmospheric interaction should be caused resulting from oblique impacts with the size smaller than the atmospheric scale height [e.g., 4, 5, 6, 7, 8]. Such atmospheric interactions between a downrange moving vapor cloud and an ambient atmosphere may have played an important role in a number of geologic events, such as the origin of the run-out flow around craters on Venus [9], massive atmospheric-blow off on the early Earth [8], and the prebiotic synthesis of highly reactive carbon radicals including CN and C_2 [6, 10]. However, the physical and chemical processes during the downrange motion have not been understood well because the controlling physics of multi-phase hypersonic flow (fine-grained fragments and gases produced by aerodynamic ablation) is significantly complicated.

In this study, we conducted high-speed imaging observations of a downrange moving vapor cloud in a gas to understand the equations of motion of the vapor cloud.

Experiments: We carried out oblique impact experiments using a two-stage light gas gun at ISAS /JAXA. An experimental chamber was filled with a nitrogen gas with the pressure of 30 hPa. We simulated the atmospheric interaction between a projectile fragments and the surrounding gas in the laboratory. A downrange moving vapor cloud was observed through acrylic view ports on the above and side of the chamber, i.e., from 2 directions perpendicular to the projectile trajectory, using 2 high-speed framing cameras with the frame rate of 1-2 μs (NAC UltraCam and Shimadzu HPV-1). A polycarbonate sphere (7 mm in diameter) and a copper plate (2×10×10 cm) were used as projectile and target, respectively. An aluminum witness plate (1.2 mm in thickness) was set 580 mm behind the impact point. Impact velocity and angle were 4.1-6.9 km/s and 30° from horizontal, respectively.

Experimental Results: Here, we describe the obtained results, such as the shape of the vapor cloud observed from the above and side view, the time evolution of the thickness of the vapor cloud and the travel dictance of the leading edge of the vapor cloud, and the downrange moving velocity immediately after the impact. Figure 1a shows the top view of the vapor cloud. The vapor cloud expands into the surrounding gas and moved to the downrange from the impact point, simultaneously, i.e., the vapor cloud was like an downrange-moving expanding disk. Figure 1b shows the time-added image of the all top view images. The clear radial streaks from the impact point are observed, suggesting that the dispersion angle of the vapor cloud from the impact point is a constant. We measured the dispersion angle as ~90° based on the crater distribution on the witness plate and the distance between the plate and the impact point. These craters also indicate that fine-grained fragments were existed in the vapor cloud. Figure 1c shows the side view of the vapor cloud. We found that the downrange-moving vapor cloud with an arrowhead shape moved around the ground, i.e., the vapor cloud did not have the momentum of vertical direction to the ground. The angle of the cusp of the angular shape was nearly constant measured as ~50°. We measured the thickness, h, of the vapor cloud as a function of time. Note that the thickness of the vapor cloud approaches an constant value, which is ~4 times the projectile diameter. Figure 2 shows the travel distance from the impact point of the leading edge of the vapor cloud as a function of time. The downrange moving velocity, v, as a function of time can be derived from the result, showing that the downrange moving projectiles were rapidly accelerated immediately after the impact to 1.3-1.9 times the impact velocities. To satisfy the energy conservation law, the upper limit of the mass of the downrange moving vapor cloud should be lower than 60-25 % of the mass of the projectile.

Discussion and Conclusion: Here, we construct a simple physical model for downrange moving vapor clouds with a disk-like shape based on the experimental results. In general, hydrodynamic deceleration from a surrounding gas, which is proportional to v^2, is dominant force for a moving object if Reynolds number, R_e, is large enough to neglect the force by the viscosity of the surrounding gas. Under our experimental condition, R_e is roughly estimated to be $>10^4$. Thus, hydrodynamic deceleration was expected to be domi-

nant force for the vapor cloud. In this case, the equations of motion of a vapor cloud is describes as

$$m dv/dt = -1/2\ \rho_a S C_D v^2,$$

where m, S, C_D and ρ_a are the mass of center-of-mass system of the cloud, the cross section for hydrodynamic force from the surrounding gas, the drag coefficient, and the density of the sorrounding gas, respectively. Based on our results, the cross section S is given as a function of time to be

$$S = h \times \{2d[\mathrm{mm}] \times \tan(45°)\},$$

where d is the travel distance from the impact point. Thus, the travel distance of the center-of-mass is solely controlled by one parameter, m/C_D. We found that there is appropreate constant value for m/C_D, which reproduces well the obtained travel distance of the leading edge of the vapor cloud (RMS is smaller than ~0.1%) as shown in Figure 2. The drag coefficient, C_D, for flying disks with an arrowhead shape observed from the side view is likely to be smaller than 1.3 estimated based on the shape and R_e dependence on C_D in a literature [11]. Thus, the maximum of the mass of the center-of-mass system can be calculated. Figure 3 shows the mass as a function of impact velocity (blue) along with the upper limit of the mass given by the energy conservation law as mentioned above (red). The mass predicted by the model is smaller than the upper limit. This comparison supports the validity of our physical model. This result indicates that the vapor cloud moves to downrange as one with a constant mass nevertheless complex physical and chemical processes,

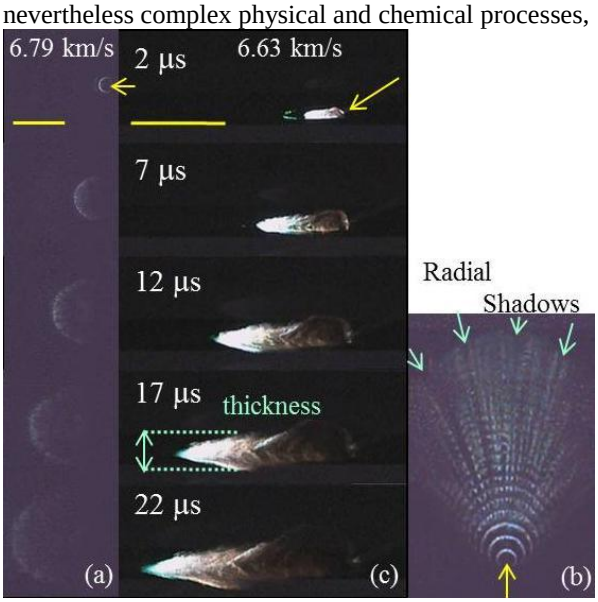

Figure 1. High-speed images of the downrange moving vapor cloud from the above (a) and the side (c). The yellow arrows indicate the impact direction. Time after the impact and 10 cm scale bar are shown in the figure. The time-added image of the all images from the above(c).

such as fragmentation and vaporization due to aerodynamic ablation, should occur in the vapor cloud. Although the applicability of the results obtained at a laboratory to actual meteoritic impact phenomena still needs more discussion, we may be able to estimate the comprehensive results after oblique impacts, such as the travel distance of vapor clouds, the swept mass of an ambient atmosphere due to the passage of the vapor cloud, the net heating rate of the vapor cloud from the colliding atmosphere, and the deposition area of highly reactive carbon radicals based on the simple physical model.

References: [1] Basaltic Volcanism Study Project. (1981) *Basaltic Volcanism on the Terrestrial Planets*, Lunar and Planetary Inst. 1049 [2] Shoemaker (1962) *Physics and Astronomy of the Moon*, Academic Press, 283. [3] Schultz and Gault (1990) *Spec. Pap. Geol. Soc. Am. 247*, 239. [4] Sugita and Schultz (2003a) *JGR, 108*, 5051. [5] Sugita and Schultz (2003b) *JGR, 108*, 5052. [6] Sugita and Schultz (2009) *GRL, 36*, L20204. [7] Schultz et al. (2006) *Int. J. Impact Eng., 33*, 771. [8] Shuvalov (2009) *MAPS, 44*, 1096. [9] Sugita and Schultz (2002) Icarus, *155*, 265. [10] Kurosawa et al. (2008) LPS XXXIX, #2037. [11] Kubota et al. (2002) *Aerodynamics of Space Vehicles*, in Japanese.

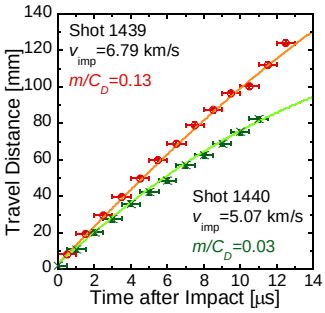

Figure 2. The travel distance of the leading edge of the vapor cloud as a function of time. Impact velocity and obtained value of m/C_D are described in the figure. The two solid lines are the prediction by the model descussed in the text.

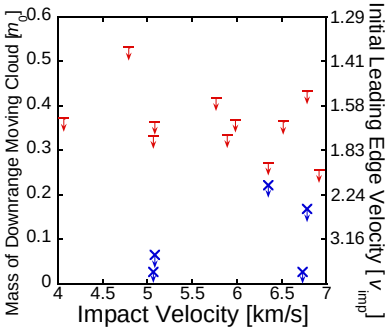

Figure 3. The estimated maximum mass normalized by the projectile mass, m0, of the downrange moving vapor cloud as a function of impact velocity (Blue cross). The upper limits of the mass defined by the energy conservation law are also indicated in the figure (Red bar). The vertical axis on the right side is the measured downrange moviong velocity immediately after the impact.